IBRACON Structures and Materials Journal
Revista IBRACON de Estruturas e Materiais
ISSN 1983-4195 ismj.org

ORIGINAL ARTICLE

Quality control tests of fresh 3D printable cement-based materials

Testes de controle de qualidade de materiais frescos à base de cimento para impressão 3D

Paulo Ricardo de Matos[a]
Hellen Prigol[a]
Adilson Schackow[a]
Samara da Silva Nazário[a]
Gabriel Doerner[a]
Nicollas Safanelli[a]

[a]Universidade do Estado de Santa Catarina – UDESC, Departamento de Engenharia Civil, Joinville, SC, Brasil

Received 02 March 2024
Revised 25 March 2024
Accepted 27 March 2024

Abstract: Three-dimensional concrete printing (3DCP) has emerged as a promising solution for the modernization of the construction sector. Additionally, design optimization allows for material reduction, promoting sustainable construction. Despite these advancements, there is still no standard for the assessment of the fresh state and quality control of 3DCP. This work discusses the results of quality control tests for fresh 3DCP. Specifically, seven samples with different mix designs were produced and subjected to rotational rheometry, slug tests, flow table tests, and buildability tests (*i.e.*, the height supported prior to collapse). The results showed that the yield stress obtained from rheometry and the slug test did not match but fell within the same order of magnitude. The yield stress values obtained from rheometry were the closest to the gravity-induced stress in the buildability test. Regarding buildability prediction, the slug test exhibited the strongest correlation with the number of layers supported in buildability (R^2 = 0.92); rotational rheometry also demonstrated a good correlation with that parameter (R^2 = 0.80). In contrast, the results of the flow table test neither correlated with the yield stress obtained from any other tests nor proved efficient in predicting buildability. Finally, the paper presented a discussion on testing and printing challenges.

Keywords: 3DCP, concrete, 3D printing, rheology, quality control.

Resumo: A impressão tridimensional de concreto (I3DC) tem se destacado como uma solução promissora para a modernização do setor da construção. Adicionalmente, a otimização do design permite a redução de materiais, promovendo a construção sustentável. Apesar desses avanços, ainda não existem normas para a avaliação do estado fresco e controle de qualidade do I3DC. Este trabalho discute os resultados de testes de controle de qualidade no estado fresco para I3DC. Especificamente, sete amostras com diferentes composições foram produzidas e submetidas a reometria rotacional, *slug test*, mesa de espalhamento e teste de construtibilidade (isto é, altura suportada antes do colapso). Os resultados mostraram que a tensão de escoamento obtido pela reometria e pelo *slug test* não coincidiram, mas estiveram dentro da mesma ordem de grandeza. Os valores da tensão de escoamento obtidos pela reometria foram os mais próximos da tensão induzida pela gravidade no teste de construtibilidade. Em relação à previsão da construtibilidade, o *slug test* apresentou a correlação mais forte com o número de camadas suportadas (R^2 = 0,92); a reometria rotacional também demonstrou uma boa correlação com esse parâmetro (R^2 = 0,80). Em contraste, os resultados do teste de mesa de espalhamento não se correlacionaram com o a tensão de escoamento obtido por nenhum outro teste e não se mostraram eficientes na previsão da construtibilidade. Finalmente, o artigo apresentou uma discussão sobre os desafios nos testes e impressão.

Palavras-chave: I3DC, concreto, impressão 3D, reologia, controle de qualidade.

How to cite: P.R. de Matos, H. Prigol, A. Schackow, S.S. Nazário, G. Doerner, N. Safanelli "Quality control tests of fresh 3D printable cement-based materials" *Rev. IBRACON Estrut. Mater.*, vol. 17, no. 5, e17515, 2024, https://doi.org/10.1590/S1983-41952024000500015.

Corresponding author: Paulo Ricardo de Matos. E-mail: paulo.matos@udesc.br
Financial support: CNPq under the projects 403563/2021-6 (Chamada CNPq/MCTI/FNDCT Nº 18/2021) and 305524/2023-2 (Chamada CNPq Nº 09/2023).
Conflict of interest: Nothing to declare.
Data Availability: Data will be made available on request.

This is an Open Access article distributed under the terms of the Creative Commons Attribution License, which permits unrestricted use, distribution, and reproduction in any medium, provided the original work is properly cited.

1 INTRODUCTION

Three-dimensional concrete printing (3DCP) has emerged as a transformative approach in the field of civil engineering. This promising technique allows for the construction of complex, formwork-free structures with increased material usage efficiency. This technology has the potential to revolutionize traditional construction methods, offering great design flexibility while reducing material waste. In addition, designed optimization allows for dematerialization and consequently more sustainable construction [1,2], well aligned with major goals for carbon emission reduction. In fact, recent studies demonstrated that 3D-printed layout-optimized concrete elements can support over 80% more load while using 1/3 less material [3].

In recent years, many studies demonstrated the advantages of 3DCP. De Schutter et al. [4] addressed the technical, economic and environmental potentials of digital construction with concrete. In summary, the authors showed that digital fabrication becomes more advantageous – from both economical and environmental points of view – as the complexity of the concrete elements increases. Wangler et al. [5] pointed out that concrete element specification (3D printed or not) must consider the interaction between structural function, material's features, process, and the shape of the element; digital fabrication can open a range of possibilities for each one of these points. Flatt and Wangler [6] discussed sustainability in digital concrete fabrication. In addition to the shape efficiency already mentioned, the authors demonstrate the potential of producing printable concrete with up to 50-60% cement replacement levels. In this regard, Zhang et al. [7] reviewed the mix design of 3DCP, assessing the composition of 22 concretes. The weight proportions of binder, water, and aggregate ranged between 600-1060, 135-365 and 820-1420 kg/m^3, respectively. Such high binder content values suggest that 3DCP mix design still must advance in terms of reducing the binder consumption to effectively reach the sustainable potential offered by such technique. This can be achieved by either replacing cement with supplementary cementitious material or by reducing the overall binder content (*e.g.*, increasing the aggregate fraction) while maintaining adequate rheological features.

Successful 3DCP construction – just like regular construction – relies on quality control. Mechtcherine et al. [8] discussed specifications in characterizing the properties of 3DCP in their hardening and hardened states. The authors highlighted the key properties to be assessed: physical (*e.g.*, density), mechanical (*e.g.*, compressive and tensile strength, and modulus of elasticity), durability (*e.g.*, chloride and carbonation resistance), and shrinkage/creep-related properties. Sample preparation and testing conditions were also discussed. As for the fresh state, one of the most important properties of 3DCP is its ability to support successive layer deposition, referred to as buildability, directly related to the maximum printable height [9]. This property is governed by the material's rheology – mainly the yield stress – both during printing (ensuring proper layer deposition) and over time (accounting for the structuration that facilitates the support of successive layers). This makes evident the practical interest in predicting the buildability of the material before the actual printing. Zhang et al. [10] proposed a monitoring method coupled with a feedback adjustment system (with computer vision and serial communication) for real-time quality control of 3DCP. For this purpose, an accelerator admixture was added near the nozzle for rheology control. Harbouz et al. [11] assessed four 3DCP mixes under rheological measurements namely "up and down" flow curves (measuring the hysteresis loop), static yield stress through stress growth test, viscoelastic measurements through small amplitude oscillatory shear, and actual 3D printing tests. The authors concluded that the well-known parameter A_{thix} was not enough to characterize the thixotropic behavior of the material since it is related to the structuration during rest, while the time-dependent behavior during shear was better characterized through a new thixotropy index proposed by them.

Although 3DCP is an emerging technology, with multi-story buildings being constructed [12], there is still no standard addressing quality control of fresh material. There is an international effort to advance on this topic, as evidenced by the existence of the RILEM Technical Committees 303-PFC "Performance requirements and testing of fresh printable cement-based materials", where some potential practical tests are being validated [9], [13]. In this regard, Rehman et al. [14] presented a critical comparison of ten inline and offline tests for quality control tests of fresh 3DCP, including rheometry, compression (uniaxial strength and squeeze flow), penetration test, ultrasound, conventional tests (slump and flow table test) and the slug test. The authors assessed the suitability of the tests based on performance parameters related to portability, economy, amount of labor involved, amount of material required, robustness of instrument, automation, and capacity of inline measurement. Overall, the structural build-up of 3DCP was better evaluated through the squeeze flow and penetration tests, followed by rheometry. In turn, the standard fresh mortar/concrete fresh-state tests (*i.e.*, flow table and slump), besides ultrasound, were the least suitable for that purpose. Despite the existence of these works, there is still no existing Brazilian literature discussing such quality control tests, to the best of our knowledge. This work discusses quality control test results for fresh 3DCP produced on a meter-scale printing setup in Brazil.

2 MATERIALS AND METHODS

2.1 Materials

Two Portland cements were used in this work, a grey Portland cement (PC) and a white Portland cement (WPC). Silica fume (SF) and calcined clay (CC) were used as supplementary cementitious materials. SF was provided by Elkem commercially available as 920D, while CC was provided by Circlua S.A. The chemical composition (determined by X-ray fluorescence) and physical properties of the binder materials are detailed in Table 1. The mineralogical composition of the binder materials determined through X-ray diffraction and Rietveld analysis following the procedures detailed in Matos et al. [15] is shown in Table 2.

Two aggregates were used, one natural quartz sand (QS) with particle size within 600-75 µm (D_{v50} = 133 µm) mm, and quartz powder (QP) with particle size within 260-30 µm (D_{v50} = 133 µm). Three chemical admixtures were used: superplasticizer (SP) commercially marketed as ADVA 458 by GCP Applied Technologies; setting retarder (SR) commercially marketed as Recover by GCP Applied Technologies; and viscosity modifying agent (VMA) commercially marketed as Sika Pump (Sika).

Table 1. Chemical composition and physical properties of the binder materials used.

Property	PC	WPC	SF	CC
Al_2O_3 (wt%)	4.7	3.1	0.4	18.6
SiO_2 (wt%)	19.9	16.5	94.0	51.6
Fe_2O_3 (wt%)	2.5	0.1	0.4	21.7
CaO (wt%)	56.4	66.4	0.3	0.2
MgO (wt%)	2.5	0.3	2.0	0.2
SO_3 (wt%)	3.3	2.5	0.2	-
$Na_2O + K_2O$ (wt%)	0.2	0.4	1.8	<0.1
Loss on ignition - 950 ^{0}C (wt%)	10.7	10.7	-	2.2
D_v50 (µm)	13.0	10.5	0.15	9.1
Density (g/cm^3)	2.98	2.97	2.21	2.89

Table 2. Mineralogical composition of the binder materials determined by XRD-Rietveld (wt%).

Phase	PC	WPC	SF	CC
C_3S	65.0	65.9	-	-
C_2S	8.3	5.8	-	-
C_3A	5.1	2.0	-	-
C_4AF	9.1	-	-	-
Lime	0.1	0.3	-	-
Portlandite	1.9	2.1	-	-
Gypsum	0.7	1.9	-	-
Calcite	4.6	17.9	-	-
Dolomite	0.7	-	-	-
Periclase	0.9	-	-	-
Alkali sulfates*	3.2	3.0		-
Ettringite	0.3	1.2	-	-
SiC	-	-	0.2	-
Sylvite	-	-	0.3	-
Quartz	-	-	-	35.9
Kaolinite	-	-	-	9.2
Hematite	-	-	-	20.1
Amorphous	-	-	99.4	34.9

*Syngenite. goergeyite. Aphthitalite.

2.2 Mix design and sample preparation

A total of seven mixes were assessed, varying the binder content and composition (type of cement and supplementary cementitious material), the aggregate content and composition (proportion between sand and quartz powder), and the chemical admixtures combination. These mix design variations were chosen based on values reported in the literature [7]

and in previous tests that defined what is suitable for printing in this specific setup. The water/binder ratio ranged between 0.36 and 0.49 and the aggregate/binder proportion ranged between 1.20 and 1.60. SP was fixed at 0.30% over the binder weight (except for Mix B containing calcined clay, fixed at 0.36%), while the water content was adjusted to allow for printing around 10-30 layers. SR was used in contents within 0.10-0.30% over the binder weight, and VMA was used in Mix D at 0.12% over the binder weight. The mix design of the samples assessed is detailed in Table 3.

Table 3. Mix design of the samples assessed.

Material/Sample	Mix A	Mix B	Mix C	Mix D	Mix E	Mix F	Mix G
Mix composition (kg/m^3)							
Cement – PC$^{(A)}$ or WPC$^{(B)}$	773$^{(A)}$	577$^{(B)}$	749$^{(A)}$	749$^{(A)}$	749$^{(A)}$	743$^{(A)}$	664$^{(A)}$
Silica fume – SF	86	0	123	123	102	101	90
Calcined clay – CC	-	180	-	-	-	-	-
Quartz powder – QP	0	180			170	506	452
Quartz sand – QS	1030	902	1022	1022	851	506	754
Water	319	335	312	312	323	329	372
Superplasticizer –SP	2.6	2.7	2.6	2.6	2.6	2.5	2.3
Viscosity modifying admixture – VMA	-	-	-	1.1	-	-	-
Setting retarder – SR	2.6	0.9	0.9	0.9	1.7	1.7	1.5
Mix design parameters							
water/binder ratio	0.37	0.44	0.36	0.36	0.38	0.39	0.49
Aggregate/binder ratio	1.20	1.43	1.17	1.17	1.20	1.20	1.60
SP content*	0.30%	0.36%	0.30%	0.29%	0.30%	0.30%	0.30%
VMA content*				0.12%			
SR content*	0.30%	0.12%	0.10%	0.10%	0.20%	0.20%	0.20%

*over the binder weight

The samples were prepared in a 35 L capacity horizontal mortar mixer, in batches of 16 L. The mixing procedure followed the steps: *(i)* the cement and sand were mixed for 2 min; *(ii)* the water was gradually added for up to 10 min of mixing, while the SR admixture was added; *(iii)* SP was added, and the sample was mixed for another 5 min; *(iv)* SF and QP (when present) were added, and the sample was mixed for another 5 min; (v) the mixer was stopped, the sample attached to the mixer container was scraped down, and the sample was mixed for another 5 min.

2.3 Printing tests: programming, testing setup and parameters.

The printing setup used is illustrated in Figure 1. A 6-axis robotic arm (ABB IRB 4600 2.05/60) with a 2.05 m reach and a 60 kg payload was used for 3DP. The motion of the robotic arm was programmed using the RobotStudio software (ABB) with RAPID language. For pumping, a grouting machine with 1100 W power and 6 L sample capacity was used. A fixed flow rate of around 1.5 L/min was used for all the 3DP tests. A 2.0 m-long rubber hose connected the pump's stator exit to the nozzle attached to the robotic arm, and a cylindrical nozzle of 22 mm in diameter was used. The width and the height of the 3DP layers were 22 and 10 mm, respectively, and the printing speed was fixed at 75 mm/s.

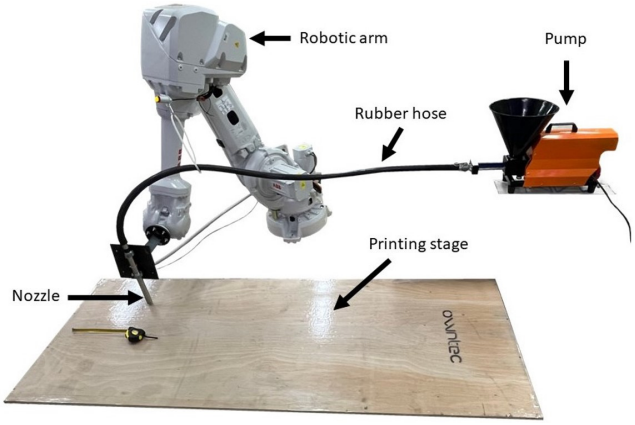

Figure 1. Setup used for 3D printing.

2.4 Quality control tests

The so-called static yield stress was obtained through rotational rheometry, conducted using a Viscotester iQ Air (Haake) rheometer with a vane tool (22.0 mm in diameter). A constant shear rate of 0.05 s^{-1} was applied for 60 seconds, and the yield stress was determined as the maximum stress resisted by the material before flowing. Three independent samples were measured for each mix.

The slug test was performed by computing the mass of 25 slugs using a digital scale, as illustrated in Figure 2. The yield stress was calculated using Equation 1 proposed by Ducoulombier et al. [16], where τ_0 is the yield stress (Pa), g is the gravitational constant (m/s^2), m is the average mass of the slugs (kg), and S is the area of the nozzle (m^2). The test was recorded in video, which also allowed for the determination of variability (mean ± standard deviation) within each 25-slug set (see Section 3.1). Two independent samples were submitted to the slug test for each mix.

$$\tau_0 = \frac{g.m}{\sqrt{3}.S} \tag{1}$$

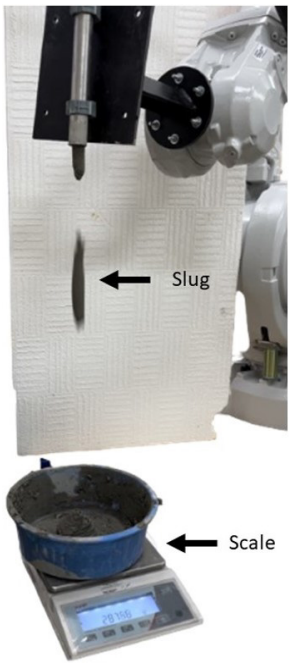

Figure 2. Setup for the slug test.

The flow table test prescribed by NBR 13276 [17] was also performed. After filling and lifting the mold with mortar, 10, 20, 30 drops of the table were applied and the mean value of two perpendicular spread measurements was recorded. This test was chosen because it is the regular test for assessing the flowability of mortar in most standards, besides being previously used for 3DCP assessment [18].

Finally, the yield stress of the mixes was assessed by the maximum number of layers that the material supports before collapsing, also referred to as buildability. For this purpose, an element with a square section of 150 mm edge was printed (see Figure 11), resulting in a time gap (*i.e.*, time between the deposition of two successive layers) of 8 seconds. The yield stress was calculated using Equation 2, where ρ is the density of the material (kg/m^3), and h is the height of the printed specimen before the collapse (m). The test was recorded in video to improve the accuracy of the measurement.

$$\tau_0 = \frac{\rho g h}{\sqrt{3}} \tag{2}$$

3 RESULTS AND DISCUSSION

3.1 Quality control test results

Table 4 details the results of the quality control tests for fresh 3DCP. All the mixes allowed for printing 10-33 successive layers. Figure 3 shows the shear stress vs. time curves obtained by rotational rheometry. One can see a relatively low variability, with a coefficient of variation usually ranging within 1-4%. As for the slug test, the repeatability was assessed by recording the individual value of each slug in two tests for Mix A, at two different times (30 and 90 min after starting mixing); the results are summarized in Figure 4. Analysis of variance – ANOVA (0.05 significance) with Tukey *post hoc* (F = 44.4574) indicated that T1_01 and T1_02 had no significant difference (p = 0. 5424) as well as T2_01 and T2_02 (p = 0. 8298). In contrast, T1_01 had a significant difference from T2_01 (p < 0.0000) and T2_02 (p < 0.0000), as well as T2_01 with T2_01 (p < 0.0000) and T2_02 (p < 0.0000). This confirms that the slug test was statistically sensible to measure the difference between the yield stress of Mix A at the two measurement times.

Table 4. Results of the quality control tests for fresh 3DCP. Note: values in parentheses correspond to the standard deviation (n = 2-3).

Mix/Test	Slug (Pa)		Vane (Pa)		Flow table (mm)						Buildability	
					10 drops		20 drops		30 drops		Layers	$\tau_{0\ (Pa)}$
Mix A	517	(28)	644	(22)	-		-		-		10	1253
Mix B	931	(118)	2054	(55)	175.0	(0.0)	207.5	(2.5)	225.0	(5.0)	19	2344
Mix C	593	(22)	1462	(37)	173.5	(1.5)	199.5	(1.5)	216.5	(1.5)	14	1735
Mix D	579	(31)	1555	(35)	205.0	(0.0)	225.0	(0.0)	237.5	(2.5)	15	1878
Mix E	665	(0)	913	(31)	208.0	(0.0)	238.0	(2.0)	257.5	(4.5)	13	1619
Mix F	1249	(27)	2613	(21)	184.0	(1.0)	213.5	(1.5)	230.0	(0.0)	33	4093
Mix G	653	(9)	1468	(56)	205.0	(0.0)	235.0	(0.0)	250.0	(0.0)	16	2117

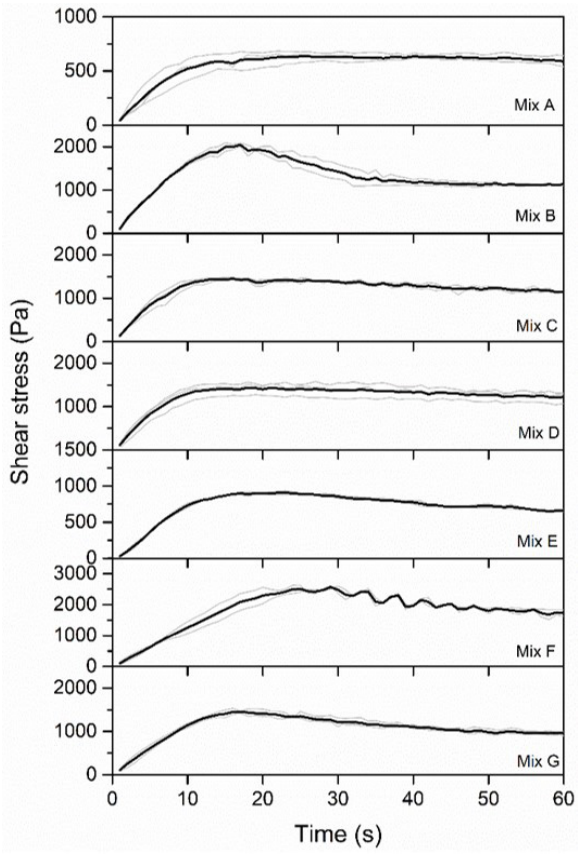

Figure 3. Shear stress vs. time curves obtained through rotational rheometry. Note: grey lines correspond to individual measurements while black lines correspond to the mean curves.

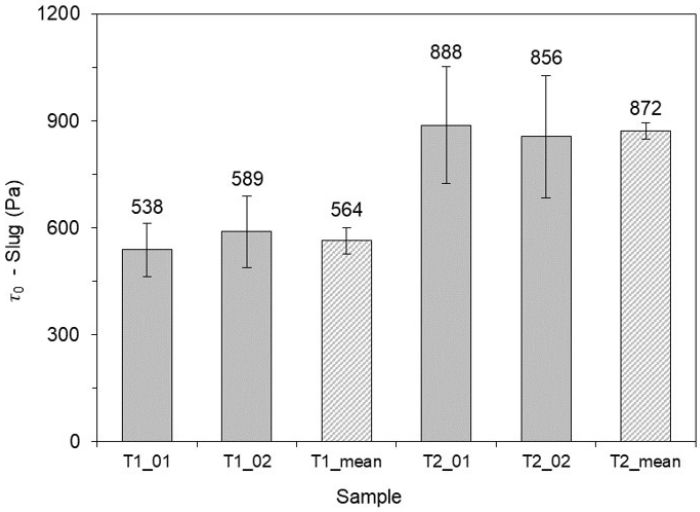

Figure 4. Repeatability of the slug test. Note: results for the Mix A at two different times: T1 = 30 min; T2 = 90 min. Error bars correspond to the standard deviation (n = 25 for "01" and "02" samples; n = 2 for "mean" samples).

Figure 5 shows the correlation between the yield stress values obtained from rotational rheometry (vane) and the slug test. The yield stress values ranged b 517-2613 Pa for the vane and slug tests. This is consistent with the minimum yield stress of 500 Pa required for proper buildability reported by Tramontin Souza et al. [19]. Rheometry led to yield stress values from 25% to 183% higher than the slug test (see Table 4), similar to that reported by Rehman et al. [14]. Nonetheless, the values obtained from the two tests had a high correlation (R^2 = 0.77). Figure 6 shows the correlation between the sample spread at the flow table test and the yield stress obtained by rotational rheometry and the slug test. It is known that the sample spread is related to the yield stress of the material. This property can be interpreted as the maximum stress resisted by the material before flowing, or the minimum stress required to start the flow. However, this correlation is well established for spread measurements under the material's weight without applying external energy such as table drops. On the contrary, when the samples present practically no spread when submitted to their weight (in practice, requiring drops to allow for spread measurement), the yield stress is no longer correlated with the sample spread, as previously demonstrated by Matos et al. [20].

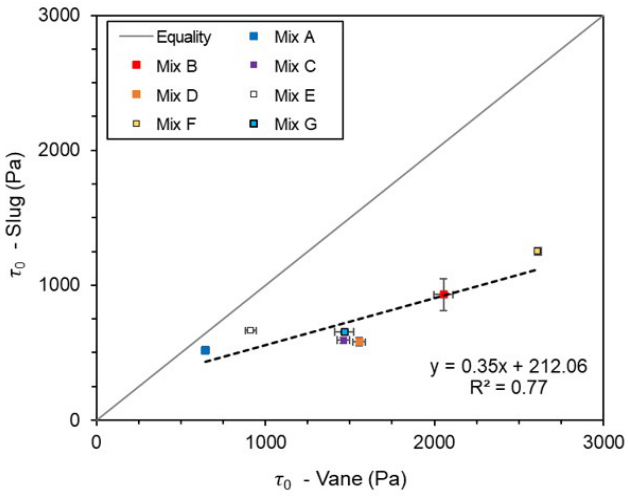

Figure 5. Correlation between the yield stress (τ_0) obtained by rotational rheometry – vane and the slug test. Error bars correspond to the standard deviation of the measurements (n = 2-3).

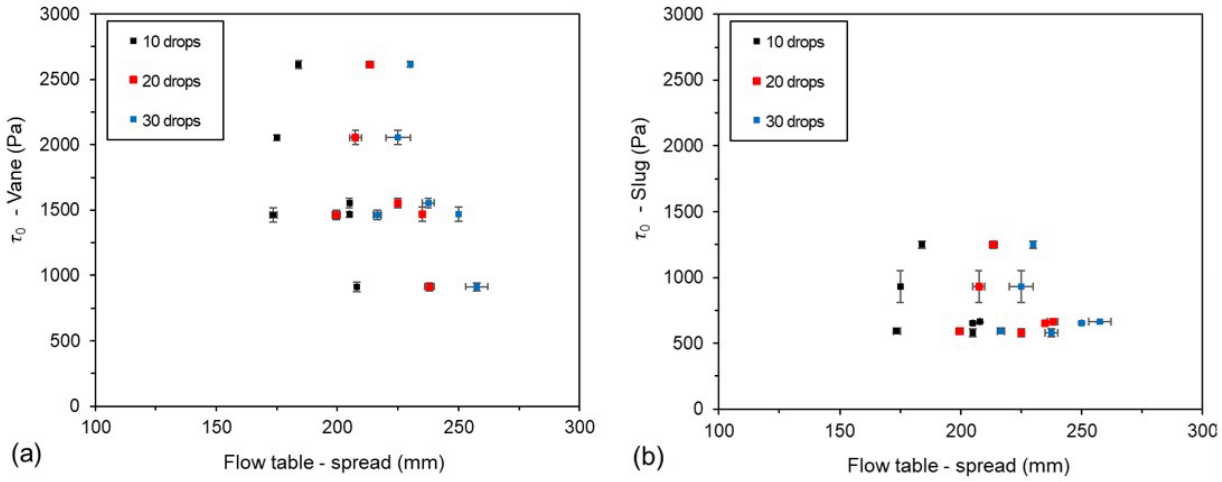

Figure 6. Correlation between the sample spread in the flow table and the yield stress (τ_0) obtained by rotational rheometry – vane (a) and the slug test (b). Error bars correspond to the standard deviation of the measurements (n = 2-3).

3.2 Buildability prediction methods

Being able to predict the number of printable layers is of great interest in the context of 3DCP. Figure 7 shows the correlation between the number of layers supported by the material before collapsing and its yield stress measured by the vane and the slug tests. High correlations were found in both cases; nonetheless, the slug test had the strongest correlation, with $R^2 = 0.90$. This indicates that the slug test was the most efficient in predicting the number of printable layers.

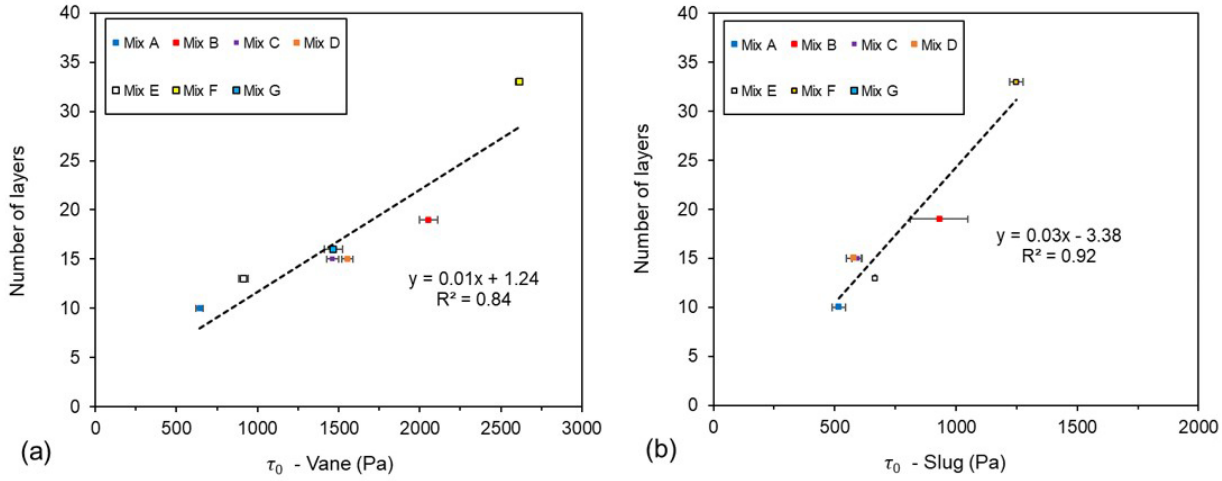

Figure 7. Correlation between the number of layers supported by the material and its yield stress (τ_0) obtained by rotational rheometry – vane (a) and the slug test (b). Error bars correspond to the standard deviation of the measurements (n = 2-3).

Figure 8 shows the correlation between the yield stress from the buildability test calculated using Equation 2 and those obtained in the rheometry and slug tests. Although the slug test led to a stronger correlation ($R^2 = 0.90$, compared to $R^2 = 0.83$ for the correlation with the vane test), rheometry led to closer values of yield stress when compared to those obtained by direct printing, *i.e.*, buildability. This indicates that despite the slug test being more efficient in predicting the number of successively printable layers, rotational rheometry led to more realistic values of real applications.

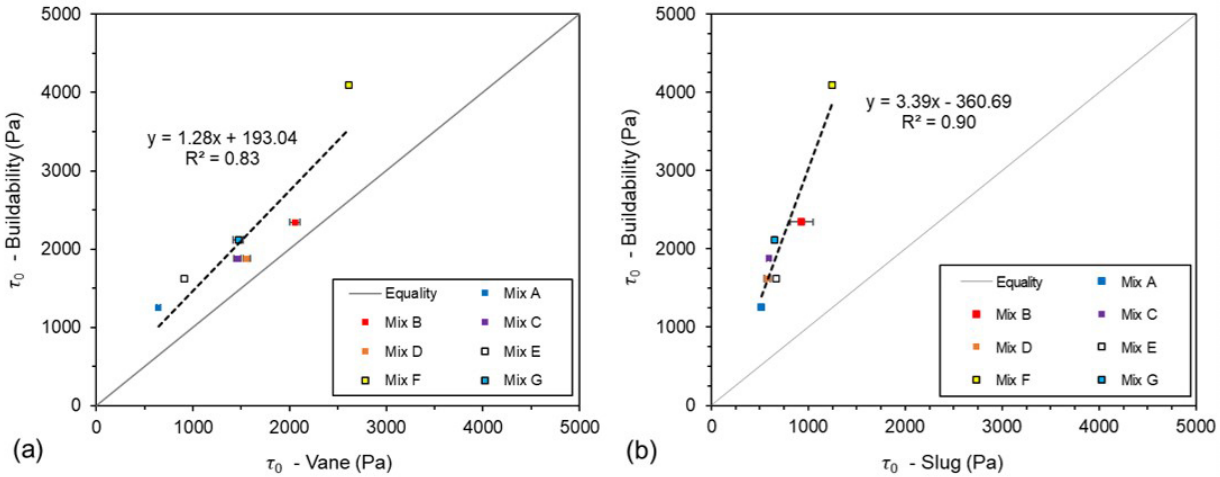

Figure 8. Correlation between the yield stress (τ_0) obtained by the buildability test and the rotational rheometry – vane (a) and the slug test (b). Error bars correspond to the standard deviation of the measurements (n = 2-3).

Finally, the sample spread of the mixes in the flow table is shown in Figure 9, as a function of the number of layers supported by the material before collapsing. No clear trend was observed between these two variables. Although the flow table is the standard test for evaluating the flowability of mortar in most standards, it was not efficient in predicting buildability for either number of drops adopted. This is consistent with that reported by Rehman et al. [14], who found that the flow table was among the less suitable tests to assess the quality control of fresh 3DCP. This can be related to the yield stress prediction of this test when the sample does not flow under its weight, as previously discussed.

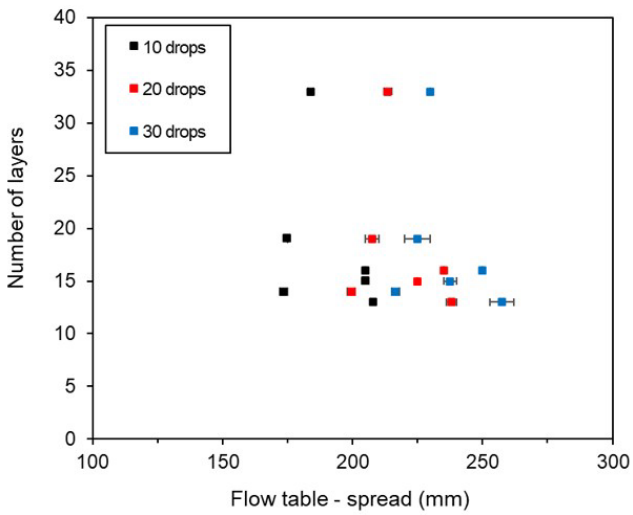

Figure 9. Flow table spread of the samples as a function of the number of layers supported, for 10, 20 and 30 drops.

3.3 Limitations in quality control tests

The quality control test results must be carefully interpreted, depending on the conditions under which the test is conducted. It is important to emphasize that fresh concrete undergoes structuration over time, increasing its yield stress and modulus of elasticity. This is a combined effect of flocculation (reversible) and progress in hydration (irreversible) [21]. Table 5 shows the fresh state test results for Mix A measured at 5 and 80 min after mixing. For the vane test, fresh 3DCP mix was placed in six cups just after mixing and three of them were tested at each age. At 5 min of age, the two tests showed yield stress values at the same order of magnitude (a difference of 25%). However, the vane yield

stress increased by 162% from 5 to 80 min while the slug test's yield stress increased by 54% within this period. This can be attributed to the fact that the vane test measured the yield stress at an undisturbed state where the reversible fraction of structuration (*e.g.*, flocculation) was not broken, while the slug test is conducted by pumping the material and consequently disturbing flocculation. Thus, despite the tests being conducted at the same age, the samples were subjected to different conditions so their results should be interpreted differently: the vane test (with the sample at rest) represents the rheological response of the material already deposited, while the slug test describes the pumping and extrusion behavior of the material.

Table 5. Fresh state test results for Mix A at different ages after mixing. Note: values in parentheses correspond to the standard deviation (n = 2-3).

Testing age	Slug (Pa)		Vane (Pa)	
5 min	517	(28)	644	(22)
80 min	795	(23)	1687	(16)

Although both vane and slug tests had good correlations with the number of layers supported in the buildability test, there are limitations in using those tests for large-scale printing quality control. In field-scale 3DCP, a reasonable time gap can be estimated as around 10 min [22]–[24] while this time in laboratory buildability test usually corresponds to a few seconds (here, 8 s). Figure 10a shows the (vane) yield stress over time of a paste produced with PC and a w/c ratio = 0.38 without SP, together with the number of layers supported in the buildability test calculated using the correlation presented in Figure 7a. The fresh paste was poured into nine different cups for individual measurements so that the yield stress could be measured without disturbance, representing the rheological behavior of layers already deposited in 3DCP. Measurements started 10 min after filling the cups, simulating the time elapsed before the gravity-induced loading in the first printed layer promoted by the second layer for the time gap fixed. The yield stress increase over the first 90 min was well described by a linear fit (R^2 = 0.95), and the slope of this fit is interpreted as the structuration rate parameter A_{thix} [25] which in this case was 6.27 Pa/min. Similarly, the structuration rate in terms of supported layers was 0.06 layer/min. This means that the fresh material would support one extra layer every ~16 min thanks to structuration, which is not considered in quick laboratory buildability tests. Thus, for accurate buildability prediction, the test should be conducted with a deposition rate compatible with that used in field applications.

In this context, A_{thix} drives the printability requirements in terms of printing speed and/or time gap. Figure 10b shows the supported number of layers over time as a function of the deposited number of layers (the latter, for a time gap of 10 min); the measured data correspond to the calculated values shown in Figure 10a while de "required" data was calculated with an A_{thix} that matched the deposition ratio, *i.e.*, 1 layer every 10 min. One can note that the sample would collapse in the 4th deposition since the structuration rate of 0.6 layer every 10 min is lower than the deposition ratio of 1 layer every 10 min. In this case, a minimum A_{thix} = 0.09 layer/min would be required to ensure continuous printing during the period assessed (*i.e.*, 90 min) or A_{thix} = 0.10 layer/min for longer periods, which corresponds to the deposition ratio.

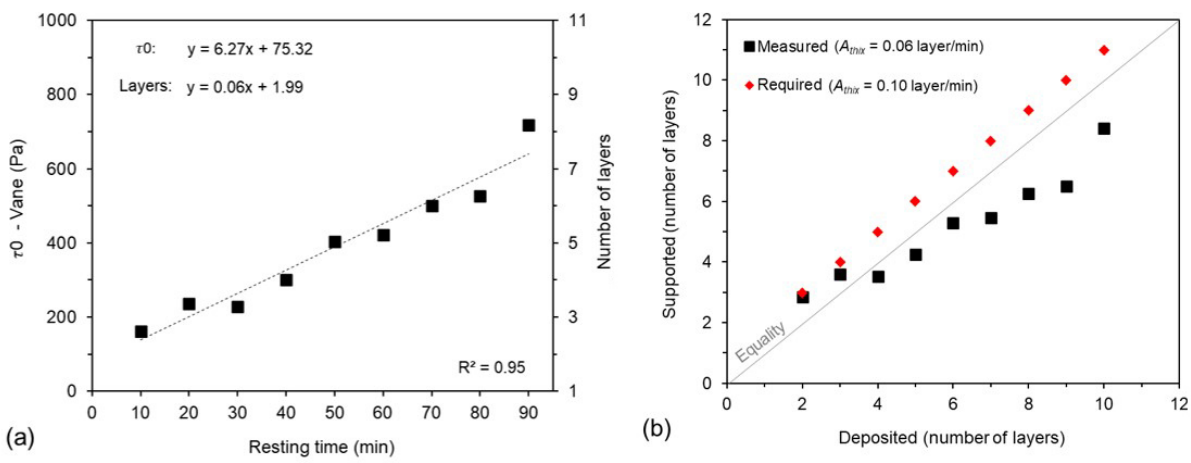

Figure 10. Fresh performance of a PC paste with w/c ratio = 0.38 without SP. (a) yield stress (obtained through rotational rheometry) and predicted number of layers over time; (b) supported vs. deposited number of layers for a time gap = 10 min.

3.4 Printing challenges and examples

Among the challenges encountered during 3DCP, ensuring a continuous material feed to the printing nozzle is a critical factor. For this purpose, the setup must rely on an adequate pumping system that provides a continuous material flow, while the printing speed (*i.e.*, the nozzle moving speed) should be compatible with the fresh material flow rate. Many mortar pumps are currently available in the market – for instance, those used for grouting or spraying – delivering flow rates ranging from less than 1 to over 50 L/min. The choice of the pumping system must be compatible with the printing speed, nozzle size, and the scale of the element to be printed. Figure 11a illustrates a layer deposition with dissonant printing speed + extrusion rate; the low extrusion rate and/or high nozzle moving speed may cause uneven material deposition and cracks from material dragging [26].

In addition to the printing setup, an appropriate mix design with tailored rheology is essential to ensure proper printing. The fresh mix should have an adequate/moderate viscosity that allows for pumping, while its yield stress must be compatible with the height of the printed element (as discussed in Section 3.2) and ensure shape retention [27]. Time-resolved rheology is also relevant, where the structuration rate (or structural build-up) plays an important role in the yield stress growth over time. Such growth is favorable for the already deposited layers to support the weight of the subsequent ones. Still, in the context of time-dependent rheology, open time is the property related to the time during which a mix can be used for 3DCP [28]. It is directly related to the mix design, especially the type and content of binders and chemical admixtures. In this scenario, the setting can be either delayed, prolonging the open time, or accelerated, enabling the printing of greater heights. Finally, voids (illustrated in Figure 12) may also be a problem during printing, which can result from pumping/feeding issues.

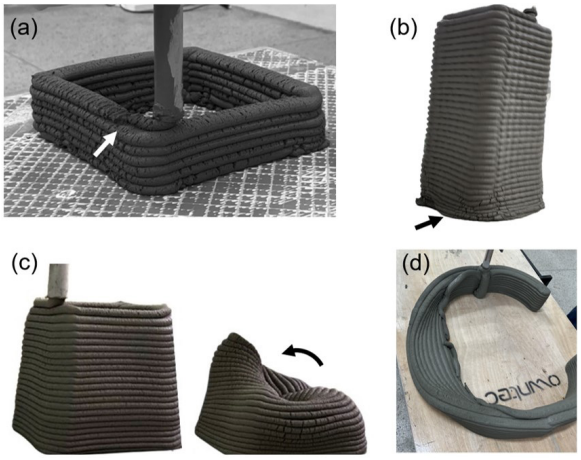

Figure 11. Failure during printing. (a) layer with cracking in fresh state; (b) plastic collapse; (c,d) elastic buckling. The arrows indicate the failure mode.

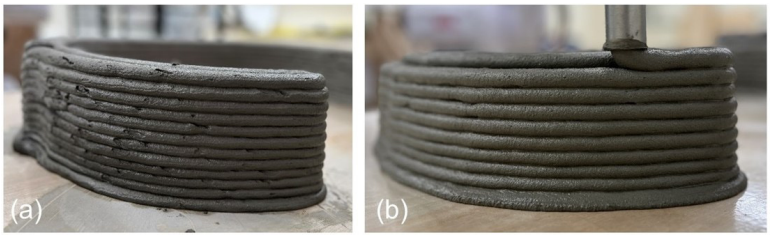

Figure 12. Examples of layer deposition with (a) and without (b) voids.

Figures 11b-d show some examples of failures during printing. In general, concrete can fail during printing due to plastic collapse (Figure 11b) or elastic buckling (Figure 11c) [29]. While the former is basically related to the material's fresh properties (especially the yield stress) and the element's height, the latter is also dependent on the element's layer thickness. In this context, thicker or multiple side-by-side layers can be chosen, increasing the inertia of the section and minimizing the occurrence of elastic buckling. Nonetheless, buckling can occur anyway – as illustrated in Figure 11d, depending on the element's geometry and fresh modulus of elasticity. Finally, by choosing an adequate mix design coupled with a proper printing setup (pump capacity, nozzle size) and proper printing parameters (printing speed, layer

height), it is possible to explore the potential of 3DCP. Figure 13 illustrates an example of a 3DCP 1-meter-long lattice specimen produced with the Mix A assessed in the current work.

Figure 13. Example of a lattice specimen printed with Mix A.

4 CONCLUSIONS

This work discussed quality control test results for fresh 3DCP. Seven samples with different mix designs were produced and subjected to rotational rheometry, slug test, flow table, and buildability tests. Based on the results obtained, the following conclusions can be drawn: *(i)* the samples exhibited yield stress values within 517-2613 Pa, allowing for printing 10-33 successive layers before collapsing; *(ii)* the yield stress obtained from rheometry and the slug test did not match but fell within the same order of magnitude. These two variables showed a linear correlation with $R^2 = 0.77$; *(iii)* the yield stress values obtained from rheometry were the closest to the gravity-induced stress in the buildability test; *(iv)* the slug test was the most effective in predicting the number of layers supported prior to collapse, exhibited a linear correlation with the buildability test result with $R^2 = 0.92$. Rotational rheometry also demonstrated a good correlation with buildability ($R^2 = 0.80$); *(v)* the flow table test neither correlated with the yield stress obtained from any other tests nor proved efficient in predicting buildability; *(vi)* the buildability test should be conducted at a deposition rate (or time gap) compatible with field application to account for the structuration of fresh cementitious material.

ACKNOWLEDGEMENTS

P.R.M. would like to acknowledge the financial support from the National Council for Scientific and Technological Development (CNPq) under the projects 403563/2021-6 (Chamada CNPq/MCTI/FNDCT Nº 18/2021) and 305524/2023-2 (Chamada CNPq Nº 09/2023). Circlua S.A. is acknowledged for providing the calcined clay used in this work.

REFERENCES

[1] L. Breseghello, H. Hajikarimian, H. B. Jørgensen, and R. Naboni, "3DLightBeam+. Design, simulation, and testing of carbon-efficient reinforced 3D concrete printed beams," *Eng. Struct.*, vol. 292, pp. 116511, 2023, http://doi.org/10.1016/j.engstruct.2023.116511.

[2] S. Maitenaz, R. Mesnil, A. Feraille, and J. F. Caron, "Materialising structural optimisation of reinforced concrete beams through digital fabrication," *Structures*, vol. 59, pp. 105644, 2024, http://doi.org/10.1016/j.istruc.2023.105644.

[3] L. Breseghello and R. Naboni, "Toolpath-based design for 3D concrete printing of carbon-efficient architectural structures," *Addit. Manuf.*, vol. 56, pp. 102872, 2022, http://doi.org/10.1016/j.addma.2022.102872.

[4] G. De Schutter, K. Lesage, V. Mechtcherine, V. N. Nerella, G. Habert, and I. Agusti-Juan, "Vision of 3D printing with concrete — Technical, economic and environmental potentials," *Cement Concr. Res.*, vol. 112, pp. 25–36, 2018, http://doi.org/10.1016/j.cemconres.2018.06.001.

[5] T. Wangler, N. Roussel, F. P. Bos, T. A. M. Salet, and R. J. Flatt, "Digital concrete: a review," *Cement Concr. Res.*, vol. 123, pp. 105780, 2019, http://doi.org/10.1016/j.cemconres.2019.105780.

[6] R. J. Flatt and T. Wangler, "On sustainability and digital fabrication with concrete," *Cement Concr. Res.*, vol. 158, pp. 106837, 2022, http://doi.org/10.1016/j.cemconres.2022.106837.

[7] C. Zhang et al., "Mix design concepts for 3D printable concrete: a review," *Cement Concr. Compos.*, vol. 122, pp. 104155, 2021, http://doi.org/10.1016/j.cemconcomp.2021.104155.

[8] V. Mechtcherine et al., "A roadmap for quality control of hardening and hardened printed concrete," *Cement Concr. Res.*, vol. 157, pp. 106800, 2022, http://doi.org/10.1016/j.cemconres.2022.106800.

[9] I. Ivanova, E. Ivaniuk, S. Bisetti, V. N. Nerella, and V. Mechtcherine, "Comparison between methods for indirect assessment of buildability in fresh 3D printed mortar and concrete," *Cement Concr. Res.*, vol. 156, pp. 106764, 2022, http://doi.org/10.1016/j.cemconres.2022.106764.

[10] H. Zhang, Y. Tan, L. Hao, S. Zhang, J. Xiao, and C. S. Poon, "Intelligent real-time quality control for 3D-printed concrete with near-nozzle secondary mixing," *Autom. Construct.*, vol. 160, pp. 105325, 2024, http://doi.org/10.1016/j.autcon.2024.105325.

[11] I. Harbouz, A. Yahia, E. Roziere, and A. Loukili, "Printing quality control of cement-based materials under flow and rest conditions," *Cement Concr. Compos.*, vol. 138, pp. 104965, 2023, http://doi.org/10.1016/j.cemconcomp.2023.104965.

[12] 3DPrint.com, "*Construction Giant Holcim Invests in Concrete 3D Printing Leader COBOD*," https://3dprint.com/294819/construction-giant-holcim-invests-in-concrete-3d-printing-leader-cobod/ (accessed Mar. 2, 2024).

[13] R. Nicolas et al., "Assessing the fresh properties of printable cement-based materials: high potential tests for quality control," *Cement Concr. Res.*, vol. 158, pp. 106836, 2022., http://doi.org/10.1016/j.cemconres.2022.106836.

[14] A. U. Rehman, A. Perrot, B. M. Birru, and J. H. Kim, "Recommendations for quality control in industrial 3D concrete printing construction with mono-component concrete: a critical evaluation of ten test methods and the introduction of the performance index," *Dev. Built Environ.*, vol. 16, pp. 100232, 2023, http://doi.org/10.1016/j.dibe.2023.100232.

[15] P. R. Matos, J. S. Andrade No., R. D. Sakata, A. P. Kirchheim, E. D. Rodríguez, and C. E. M. Campos, "Strategies for XRD quantitative phase analysis of ordinary and blended Portland cements," *Cement Concr. Compos.*, vol. 131, pp. 104571, 2022, http://doi.org/10.1016/j.cemconcomp.2022.104571.

[16] N. Ducoulombier et al., "The "Slugs-test" for extrusion-based additive manufacturing: protocol, analysis and practical limits," *Cement Concr. Compos.*, vol. 121, pp. 104074, 2021, http://doi.org/10.1016/j.cemconcomp.2021.104074.

[17] Associação Brasileira de Normas Técnicas, *Argamassa para Assentamento e Revestimento de Paredes e Tetos - Determinação do Índice de Consistência*, ABNT NBR 13276, 2016.

[18] Y. W. D. Tay, Y. Qian, and M. J. Tan, "Printability region for 3D concrete printing using slump and slump flow test," *Compos., Part B Eng.*, vol. 174, pp. 106968, 2019, http://doi.org/10.1016/j.compositesb.2019.106968.

[19] M. Tramontin Souza et al., "Role of chemical admixtures on 3D printed Portland cement: assessing rheology and buildability," *Constr. Build. Mater.*, vol. 314, pp. 125666, 2022, http://doi.org/10.1016/j.conbuildmat.2021.125666.

[20] P. R. Matos, R. Pilar, C. A. Casagrande, P. J. P. Gleize, and F. Pelisser, "Comparison between methods for determining the yield stress of cement pastes," *J. Braz. Soc. Mech. Sci. Eng.*, vol. 42, no. 1, pp. 24, 2020, http://doi.org/10.1007/s40430-019-2111-2.

[21] N. Roussel, G. Ovarlez, S. Garrault, and C. Brumaud, "The origins of thixotropy of fresh cement pastes," *Cement Concr. Res.*, vol. 42, no. 1, pp. 148–157, 2012, http://doi.org/10.1016/j.cemconres.2011.09.004.

[22] G. H. Ahmed, N. H. Askandar, and G. B. Jumaa, "A review of largescale 3DCP: material characteristics, mix design, printing process, and reinforcement strategies," *Structures*, vol. 43, pp. 508–532, 2022, http://doi.org/10.1016/j.istruc.2022.06.068.

[23] S. H. Chu, L. G. Li, and A. K. H. Kwan, "Development of extrudable high strength fiber reinforced concrete incorporating nano calcium carbonate," *Addit. Manuf.*, vol. 37, pp. 101617, 2021, http://doi.org/10.1016/j.addma.2020.101617.

[24] J. G. Silveira Jr. et al., "Influence of time gap on the buildability of cement mixtures designed for 3D printing," *Buildings*, vol. 14, no. 4, pp. 1070, 2024, http://doi.org/10.3390/buildings14041070.

[25] N. Roussel and F. Cussigh, "Distinct-layer casting of SCC: the mechanical consequences of thixotropy," *Cement Concr. Res.*, vol. 38, no. 5, pp. 624–632, 2008, http://doi.org/10.1016/j.cemconres.2007.09.023.

[26] A. U. Rehman and J.-H. Kim, "3D concrete printing: a systematic review of rheology, mix designs, mechanical, microstructural, and durability characteristics," *Materials*, vol. 14, no. 14, pp. 3800, 2021, http://doi.org/10.3390/ma14143800.

[27] S. Paritala, K. K. Singaram, I. Bathina, M. A. Khan, and S. K. R. Jyosyula, "Rheology and pumpability of mix suitable for extrusion-based concrete 3D printing: a review," *Constr. Build. Mater.*, vol. 402, pp. 132962, 2023, http://doi.org/10.1016/j.conbuildmat.2023.132962.

[28] R. A. Buswell, W. R. Leal de Silva, S. Z. Jones, and J. Dirrenberger, "3D printing using concrete extrusion: a roadmap for research," *Cement Concr. Res.*, vol. 112, pp. 37–49, 2018, http://doi.org/10.1016/j.cemconres.2018.05.006.

[29] A. V. Rahul and M. Santhanam, "Evaluating the printability of concretes containing lightweight coarse aggregates," *Cement Concr. Compos.*, vol. 109, pp. 103570, 2020, http://doi.org/10.1016/j.cemconcomp.2020.103570.

Author contributions: Conceptualization, P.R.M., H.P., A.S.; methodology, P.R.M., H.P., A.S.; formal analysis, P.R.M., A.S.; investigation, P.R.M., H.P., A.S., S.S.N., G.D., N.S.; resources, P.R.M.; data curation, P.R.M., H.P.; writing – original draft preparation, P.R.M.; writing—review and editing, H.P., A.S., S.S.N., G.D., N.S.; supervision, P.R.M., A.S.; funding acquisition, P.R.M.

Editors: Bruno Briseghella, Daniel Carlos Taissum Cardoso.